

# Testing the running of non-Gaussianity through the CMB $\mu$ -distortion and the halo bias

Matteo Biagetti, Hideki Perrier, Antonio Riotto, and Vincent Desjacques

*Department of Theoretical Physics and Center for Astroparticle Physics (CAP), Université de Genève,  
24 quai Ernest Ansermet, CH-1211 Geneva 4, Switzerland*

(Received 15 January 2013; published 22 March 2013)

The primordial non-Gaussianity parameters  $f_{\text{NL}}$  and  $\tau_{\text{NL}}$  may be scale dependent. We investigate the capability of future measurements of the CMB  $\mu$  distortion, which is very sensitive to small scales, and of the large-scale halo bias to test the running of local non-Gaussianity. We show that, for an experiment such as PIXIE, a measurement of the  $\mu$ -temperature correlation can pin down the spectral indices  $n_{f_{\text{NL}}}$  and  $n_{\tau_{\text{NL}}}$  to values of the order of 0.3 if  $f_{\text{NL}} = 20$  and  $\tau_{\text{NL}} = 5000$ . A similar value can be achieved with an all-sky survey extending to redshift  $z \sim 1$ . In the particular case in which the two spectral indices are equal, as predicted in models where the cosmological perturbations are generated by a single field other than the inflaton, the  $1\sigma$  error on the scale dependence of the nonlinearity parameters goes down to 0.2.

DOI: [10.1103/PhysRevD.87.063521](https://doi.org/10.1103/PhysRevD.87.063521)

PACS numbers: 98.80.Es, 95.80.+p, 98.70.Vc, 98.65.Dx

## I. INTRODUCTION

Detecting a possible primordial source of non-Gaussianity (NG) in the cosmological perturbations is one of the main targets of current and future experiments measuring the properties of the cosmic microwave background (CMB) anisotropies and the large-scale structure of the Universe. Indeed, measuring a certain level of NG in the three- (bispectrum) and four-point (trispectrum) correlator of the perturbations opens up a unique window into the physics of inflation, which is believed to be the period during which such fluctuations are quantum-mechanically generated [1]. The current constraints on NG come from the measurement of the CMB anisotropy bispectrum [2] and from the properties of the clustering of galaxies, which have been identified to be a powerful probe of NG thanks to the fact that NG introduces a scale-dependent bias between the power spectra of halos and dark matter [3,4].

Most of the attention in the literature has been devoted to the so-called “local” model of NG, where NG is defined in terms of the primordial gravitational potential  $\Phi(\vec{x})$  as

$$\Phi(\vec{x}) = \phi_{\text{G}}(\vec{x}) + f_{\text{NL}}[\phi_{\text{G}}^2(\vec{x}) - \langle \phi_{\text{G}}^2(\vec{x}) \rangle]. \quad (1)$$

The corresponding bispectrum and trispectrum are given by

$$B_{\Phi}(k_1, k_2, k_3) = 2f_{\text{NL}}[P_{\phi}(k_1)P_{\phi}(k_2) + 2 \text{cyc.}], \quad (2)$$

$$\begin{aligned} T_{\Phi}(k_1, k_2, k_3, k_4) \\ = \frac{25}{9} \tau_{\text{NL}}[P_{\phi}(k_1)P_{\phi}(k_2)P_{\phi}(k_3) + 11 \text{cyc.}], \end{aligned} \quad (3)$$

where  $P_{\phi}(k)$  is the power spectrum of the gravitational potential. This type of NG is generated in multifield inflationary models where the cosmological perturbation is sourced by light scalar fields other than the inflaton. The corresponding perturbations are both scale invariant and special conformally invariant [5,6]. The parameter  $f_{\text{NL}}$  is

currently constrained to be in the range  $(32 \pm 21)$  by WMAP [2] and  $(28 \pm 23)$  by large-scale structure [7], while the parameter  $\tau_{\text{NL}}$  needs to be in the range  $(-0.6 < \tau_{\text{NL}}/10^4 < 3.3)$  as inferred from the WMAP five-year data [8]. Measuring the amplitudes of both the bispectrum and the trispectrum is extremely interesting as, if only one degree of freedom is responsible for the perturbations, then there is a well-defined relation between the NG parameters,  $\tau_{\text{NL}} = (\frac{6}{5}f_{\text{NL}})^2$ . By contrast, if more than one field is responsible for the cosmological perturbations generated through the inflationary dynamics, then there exists an inequality,  $\tau_{\text{NL}} > (\frac{6}{5}f_{\text{NL}})^2$  [6,9,10]. The extent to which future measurements of the scale dependence of halo bias can test multifield inequality has been the subject of Ref. [11].

Even though the definitions in Eqs. (2) and (3) are widely used to model NG in the primordial perturbations, they are just the first step one can take on this matter. One more general definition of the bispectrum and trispectrum could include a scale dependence in the nonlinearity parameters  $f_{\text{NL}}$  and  $\tau_{\text{NL}}$ . This step is well motivated by the theoretical predictions of some models [12–16]. The running with physical scale of the NG parameters  $f_{\text{NL}}$  and  $\tau_{\text{NL}}$  has been the subject of intense recent research [17–24].

To account for the running of  $f_{\text{NL}}$  in its full generality, one can adopt, for example, the parametrization used in Ref. [25] (see also Ref. [14]):

$$\begin{aligned} B_{\Phi}(k_1, k_2, k_3) \\ = 2[\xi_{f_{\text{NL}}}(k_3)\xi_m(k_1)\xi_m(k_2)P_{\phi}(k_1)P_{\phi}(k_2) + \text{cyc.}], \end{aligned} \quad (4)$$

where

$$\xi_{f_{\text{NL},m}}(k) = \xi_{f_{\text{NL},m}}(k_0) \left( \frac{k}{k_0} \right)^{n_{f_{\text{NL},m}}}. \quad (5)$$

Here,  $\xi_{f_{\text{NL}}}(k)$  parametrizes the (self-)interactions of the fields, and  $\xi_m(k)$  the ratio of the contribution of each field.

From this general parametrization, we can also easily extend the one for the trispectrum:

$$T_{\Phi}(k_1, k_2, k_3, k_4) = \frac{25}{9} [\xi_{\tau_{\text{NL}}}(k_3, k_4) \xi_m(k_1) \xi_m(k_2) \xi_m(k_{13}) \\ \times P_{\phi}(k_1) P_{\phi}(k_2) P_{\phi}(k_{13}) + \text{cyc.}], \quad (6)$$

where

$$\xi_{\tau_{\text{NL}}}(k_i, k_j) = \xi_{\tau_{\text{NL}}}(k_0) \left( \frac{k_i k_j}{k_0^2} \right)^{n_{\tau_{\text{NL}}}}. \quad (7)$$

In the single-field limit,  $\xi_{\tau_{\text{NL}}}(k_i, k_j) = \frac{36}{25} \xi_{f_{\text{NL}}}(k_i) \xi_{f_{\text{NL}}}(k_j)$  and  $\xi_m(k) = 1$ . According to this parametrization, in the case of a multifield inflation, we have three free parameters,  $n_{f_{\text{NL}}}$ ,  $n_m$  and  $n_{\tau_{\text{NL}}}$ , which describe the scale dependence of the nonlinearity parameters  $f_{\text{NL}}$  and  $\tau_{\text{NL}}$  and of the dimensionless power spectra. In order to decrease the complexity of the analysis, from now on we make the assumption that  $n_m$  is significantly much smaller than unity. By doing so, we are left with the following parametrization of the nonlinear parameters:

$$f_{\text{NL}}(k) = f_{\text{NL}}^* \left( \frac{k}{k_*} \right)^{n_{f_{\text{NL}}}} \quad (8)$$

and

$$\tau_{\text{NL}}(k_i, k_j) = \tau_{\text{NL}}^* \left( \frac{k_i k_j}{k_*^2} \right)^{n_{\tau_{\text{NL}}}}. \quad (9)$$

CMB information alone, in the event of a significant detection of the NG component, corresponding to  $f_{\text{NL}} = 50$  for the local model, is able to determine  $n_{f_{\text{NL}}}$  with a  $1\sigma$  uncertainty of about 0.1 for the Planck mission [17]. A local bias analysis performed in the same Ref. [17] showed that high-redshift surveys ( $z > 1$ ) covering a large fraction of the sky, corresponding to a volume of about  $100h^{-3} \text{ Gpc}^3$ , might provide a  $1\sigma$  error on the running  $f_{\text{NL}}$  parameter of the order of  $0.4(50/f_{\text{NL}})$ . On the other hand, using the WMAP temperature maps, a constraint on the running of the scale-dependent parameter  $f_{\text{NL}}$  has been recently obtained in Ref. [26]:  $n_{f_{\text{NL}}} = 0.30(+1.9)(-1.2)$  at 95% confidence, marginalized over the amplitude  $f_{\text{NL}}^*$ . To the best of our knowledge, no forecasts for the running of the trispectrum parameter  $\tau_{\text{NL}}$  exist in the literature. In fact, in the case in which the perturbations are sourced by a single field, a well-defined relation between the running spectral indices holds:

$$n_{f_{\text{NL}}} = n_{\tau_{\text{NL}}}, \quad (10)$$

and the indices are therefore not independent. In this paper, we will assume that  $f_{\text{NL}}$  and  $\tau_{\text{NL}}$ , and therefore their spectral indices too, are not related to each other, thus

leaving open the possibility that the perturbations originate from a multifield scenario.

The goal of this paper is to provide some useful forecasts on the spectral indices  $n_{f_{\text{NL}}}$  and  $n_{\tau_{\text{NL}}}$  from the possible physical imprints that NG can leave on the CMB  $\mu$  distortion and the halo bias. Measurements of the  $\mu$ -type distortion of the CMB spectrum provide the unique opportunity to probe these scales over the unexplored range from  $50$  to  $10^4 \text{ Mpc}^{-1}$ , and it has been recently pointed out that correlations between  $\mu$  distortion and temperature anisotropies can be used to test Gaussianity at these very small scales. In particular, the  $\mu$ -temperature cross correlation is proportional to the very squeezed limit of the local primordial bispectrum, and hence measures  $f_{\text{NL}}$ , while the  $\mu$ - $\mu$  is proportional to the primordial trispectrum and measures  $\tau_{\text{NL}}$  [27] (see also Ref. [28]). Since the  $\mu$  distortion is localized at small scales, we expect it to be very sensitive to the possible running of the NG parameters  $f_{\text{NL}}$  and  $\tau_{\text{NL}}$ . This will be studied in Sec. II. In Sec. III, we will study the effect of running NG parameters on the halo bias, taking into account the running of the trispectrum amplitude as well. Our conclusions will be presented in Sec. IV. In all illustrations, the cosmology is a flat  $\Lambda$ CDM universe with normalization  $\sigma_8 = 0.803$ , Hubble constant  $h_0 = 0.701$  and matter content  $\Omega_m = 0.279$ .

## II. CMB $\mu$ DISTORTION

The goal of this section is to compute the effect of running NG on the CMB  $\mu$  distortion. The latter is caused by the energy injection originated by the dissipation of acoustic waves through the Silk damping as they reenter the horizon and start oscillating. An interesting property is that this effect is related to primordial perturbation scales of  $50 \lesssim k \text{ Mpc} \lesssim 10^4$ , which are not accessible from CMB anisotropies observations.

At early times ( $z \gg z_{\mu,i} \equiv 2 \times 10^6$ ), the content of the Universe can be described as a photon-baryon fluid in thermal equilibrium with a blackbody spectrum. This equilibrium is achieved mainly through elastic and double Compton scattering. However, at later times ( $z_{\mu,f} \equiv 5 \times 10^4 \lesssim z \lesssim z_{\mu,i}$ ), double Compton scattering is no longer efficient, whereas single Compton scattering still provides equilibrium. The photon number density is, however, frozen, and only the frequency of the photons can be changed. It can be shown that any energy injection in the photon-baryon fluid will distort the spectrum by the creation of a chemical potential  $\mu$ . The photon number density per frequency interval is then  $n(\nu) = (e^{x+\mu(x)} - 1)^{-1}$ , where  $x \equiv h\nu/(k_B T)$ . The parameter  $\mu$  due to damping of acoustic waves can then be expressed in terms of the primordial power spectrum [29]. Using the Bose-Einstein distribution plus the fact that the total number of photons is constant, for an amount of energy (density) released into the plasma  $\delta E/E$ , one finds that  $\mu \simeq 1.4\delta E/E$ , where

$$\frac{\delta E}{E} \simeq \frac{1}{4} \langle \delta_\gamma^2(\vec{x}) \rangle_{z_{\mu,f}}^{z_{\mu,i}} \quad (11)$$

and  $\langle \delta_\gamma^2(\vec{x}) \rangle$  represents the photon energy density fluctuation averaged over one period of the acoustic oscillations. As the modes of interest reenter the horizon during the radiation phase, one finally finds

$$\mu(\vec{x}) \simeq 4.6 \int \frac{d^3 k_1 d^3 k_2}{(2\pi)^6} \zeta_{\vec{k}_1} \zeta_{\vec{k}_2} e^{i\vec{k}_+ \cdot \vec{x}} W\left(\frac{\vec{k}_+}{k_s}\right) \times \langle \cos(k_1 r) \cos(k_2 r) \rangle_p [e^{-(k_1^2 + k_2^2)/k_D^2}]_{z_{\mu,f}}^{z_{\mu,i}} \quad (12)$$

where  $\zeta(\vec{x}) = 5\Phi(\vec{x})/3$  describes curvature perturbations;  $\vec{k}_\pm \equiv \vec{k}_1 \pm \vec{k}_2$ ; and in order to account for the fact that the distortion arises from a thermalization process, one uses a top-hat filter in real space  $W(\vec{x})$ , which smears the dissipated energy over a volume of radius  $k_{D,f}^{-1} \leq k_s^{-1}$ , where  $k_D(z)$  is the diffusion momentum scale

$$k_D(z) \simeq 4.1 \times 10^{-6} (1+z)^{3/2} \text{ Mpc}^{-1}. \quad (13)$$

We proceed by computing the correlations between  $\mu$  distortion and temperature anisotropy, as well as  $\mu\mu$  self-correlation as done in Ref. [27], but allowing for a running of  $f_{\text{NL}}$  and  $\tau_{\text{NL}}$  given by Eqs. (8) and (9). The curvature perturbation bispectrum in the squeezed limit ( $k_3 \ll k_1 \sim k_2$ ) is expressed as

$$\langle \zeta_{\vec{k}_1} \zeta_{\vec{k}_2} \zeta_{\vec{k}_3} \rangle = (2\pi)^3 \delta^3(\vec{k}_1 + \vec{k}_2 + \vec{k}_3) \frac{12}{5} f_{\text{NL}}(k_-/2) \times P(k_-/2) P(k_+). \quad (14)$$

The temperature- $\mu$  correlation therefore reads<sup>1</sup>

$$C_\ell^{\mu T} = -6.1\pi \frac{9}{25} f_{\text{NL}}^* b \frac{\Delta_\zeta^4(k_p)}{\ell(\ell+1)} \ln\left(\frac{k_{D,i}}{k_{D,f}}\right) \simeq -2.2 \times 10^{-16} f_{\text{NL}}^* \frac{b}{\ell(\ell+1)}, \quad (15)$$

where the primordial curvature spectrum is defined by  $\langle \zeta_{\vec{k}_1} \zeta_{\vec{k}_2} \rangle = (2\pi)^3 \delta^3(\vec{k}_1 + \vec{k}_2) 2\pi^2 \Delta_\zeta^2(k_1)/k_1^3$  with  $\Delta_\zeta^2(k_p) = 2.4 \times 10^{-9}$  at the pivot scale  $k_p \equiv 0.002 \text{ Mpc}^{-1}$  [2]. The parameter  $b$  is defined by

<sup>1</sup>To compute the temperature anisotropies, we adopt the same approximation as in Ref. [27]; that is, the Sachs-Wolfe approximation. Based on the findings in Ref. [28], where the full radiation transfer function was adopted, we expect an overall decrease of the signal-to-noise ratio of the order of 40%. Later in the text, we also point out that the change of the pivot scale amounts to corrections of the order of 30%.

$$\frac{b}{\ell(\ell+1)} \equiv \frac{2}{\ln\left(\frac{k_{D,i}}{k_{D,f}}\right)} \int d \ln k_+ j_\ell(k_+ r_\ell)^2 W\left(\frac{k_+}{k_s}\right) \times \int d \ln k_- \left(\frac{k_-}{2k_*}\right)^{n_{f_{\text{NL}}}} \frac{\Delta_\zeta^2(k_-/2) \Delta_\zeta^2(k_+)}{\Delta_\zeta^4(k_p)} \times [e^{-k_-^2/(2k_D^2)}]_{z_{\mu,f}}^{z_{\mu,i}}. \quad (16)$$

The  $\mu$  distortion is created during the period between  $z_{\mu,i} = 2 \times 10^6$  and  $z_{\mu,f} = 5 \times 10^4$ , which implies  $k_{D,i} \simeq 11600 \text{ Mpc}^{-1}$  and  $k_{D,f} \simeq 46 \text{ Mpc}^{-1}$ . For a weak scale dependence  $\Delta_\zeta^2(k) = \Delta_\zeta^2(k_p)(k/k_p)^{n_s-1}$ , we obtain

$$b \simeq \frac{1}{\ln\left(\frac{k_{D,i}}{k_{D,f}}\right)} \frac{1}{n_s + n_{f_{\text{NL}}} - 1} \left(\frac{1}{\sqrt{2}k_p}\right)^{n_s-1} \times \left(\frac{1}{\sqrt{2}k_*}\right)^{n_{f_{\text{NL}}}} [k_D(z)^{n_s+n_{f_{\text{NL}}}-1}]_{z_{\mu,f}}^{z_{\mu,i}}. \quad (17)$$

If we take the same pivot for  $f_{\text{NL}}$  as for the primordial spectrum,  $k_* = k_p$ , the equation above becomes the same expression as for a constant  $f_{\text{NL}} = f_{\text{NL}}^*$  but with a shifted spectral index  $n_s$  replaced by  $(n_s + n_{f_{\text{NL}}})$ . This shows explicitly that we recover the scale-invariant result for  $n_{f_{\text{NL}}} = 0$ , and we have  $b \simeq 1 + 10(n_s + n_{f_{\text{NL}}} - 1)$  for  $(n_s + n_{f_{\text{NL}}} - 1) \simeq 0$ .

Using the trispectrum in the collapsed limit ( $\vec{k}_{12} \sim 0$ ),

$$\langle \zeta_{\vec{k}_1} \zeta_{\vec{k}_2} \zeta_{\vec{k}_3} \zeta_{\vec{k}_4} \rangle = (2\pi)^3 \delta^3(\vec{k}_1 + \vec{k}_2 + \vec{k}_3 + \vec{k}_4) \times 4\tau_{\text{NL}}(k_-/2, k_3) P(k_-/2) P(k_+) P(k_3), \quad (18)$$

we obtain the NG contribution to the  $\mu$ -distortion self-correlation:

$$C_\ell^{\mu\mu} = 42\pi\tau_{\text{NL}}^* \tilde{b} \frac{\Delta_\zeta^6(k_p)}{\ell(\ell+1)} \ln^2\left(\frac{k_{D,i}}{k_{D,f}}\right) \simeq 5.6 \times 10^{-23} \tau_{\text{NL}}^* \frac{\tilde{b}}{\ell(\ell+1)}, \quad (19)$$

where

$$\tilde{b} \equiv \frac{2l(l+1)}{\ln^2\left(\frac{k_{D,i}}{k_{D,f}}\right)} \int d \ln k_+ d \ln k_- d \ln k_3 j_\ell(k_+ r_\ell)^2 W\left(\frac{k_+}{k_s}\right) \times \left(\frac{k_- k_3}{2k_*^2}\right)^{n_{\tau_{\text{NL}}}} \frac{\Delta_\zeta^2(k_-/2) \Delta_\zeta^2(k_+) \Delta_\zeta^2(k_3)}{\Delta_\zeta^6(k_p)} \times [e^{-k_-^2/(2k_D^2)}]_{z_{\mu,f}}^{z_{\mu,i}} [e^{-2k_3/(2k_D^2)}]_{z_{\mu,f}}^{z_{\mu,i}} \simeq \frac{1}{\ln^2\left(\frac{k_{D,i}}{k_{D,f}}\right)} \left(\frac{1}{n_{\tau_{\text{NL}}} + n_s - 1}\right)^2 \left(\frac{1}{\sqrt{2}k_p}\right)^{2(n_s-1)} \left(\frac{1}{\sqrt{2}k_*}\right)^{2n_{\tau_{\text{NL}}}} \times ([k_D(z)^{n_{\tau_{\text{NL}}}+n_s-1}]_{z_{\mu,f}}^{z_{\mu,i}})^2. \quad (20)$$

This is just  $b^2$  with the index  $n_{f_{\text{NL}}}$  replaced by  $n_{\tau_{\text{NL}}}$ , and it corresponds to the result of a constant  $\tau_{\text{NL}} = \tau_{\text{NL}}^*$  with  $n_s$

replaced by  $(n_s + n_{\tau_{\text{NL}}})$ . We recover the scale-invariant result for  $n_{\tau_{\text{NL}}} = 0$ . The behavior of the parameters  $b$  and  $\tilde{b}$  is shown in Fig. 1.

Having computed the key parameters  $b$  and  $\tilde{b}$ , we proceed by estimating the signal-to-noise ratio to estimate the values of  $n_{f_{\text{NL}}}$  and  $n_{\tau_{\text{NL}}}$  measurable from the  $\mu$  distortion, assuming that the amplitudes  $f_{\text{NL}}^*$  and  $\tau_{\text{NL}}^*$  are known from other experiments. In general, the signal-to-noise ratio for variables  $\lambda_i$  is defined in terms of the Fisher matrix as [30]

$$\frac{S}{N} \equiv \sqrt{\lambda_i F_{ij} \lambda_j}. \quad (21)$$

In the case of only one variable, it reduces to  $S/N = \lambda \sqrt{F} = \lambda / \sigma_\lambda$ . In our case, to measure the spectral index  $n_{f_{\text{NL}}}$  we can adopt the Fisher matrix

$$F = \sum_{\ell \geq 2} \frac{1}{\sigma_{C_\ell^{\mu T}}^2} \left( \frac{\partial C_\ell^{\mu T}}{\partial n_{f_{\text{NL}}}} \right)^2, \quad (22)$$

while for the spectral index  $n_{\tau_{\text{NL}}}$  we adopt the Fisher matrix

$$F = \sum_{\ell \geq 2} \frac{1}{\sigma_{C_\ell^{\mu\mu}}^2} \left( \frac{\partial C_\ell^{\mu\mu}}{\partial n_{\tau_{\text{NL}}}} \right)^2. \quad (23)$$

The noise for  $\mu$  distortion can be modeled, assuming a Gaussian beam experiment [31], by

$$C_\ell^{\mu\mu, N} \simeq w_\mu^{-1} e^{\ell^2 / \ell_{\text{max}}^2}, \quad (24)$$

where  $\ell_{\text{max}}$  is the maximum multipole fixed by the experiment's beam size and  $w_\mu$  is the sensitivity to  $\mu$ . For the

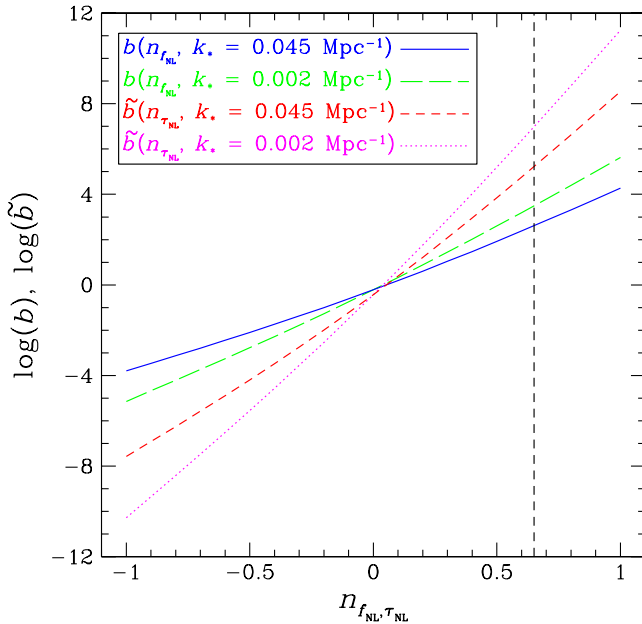


FIG. 1 (color online). Value of the parameters  $b(n_{f_{\text{NL}}})$  and  $\tilde{b}(n_{\tau_{\text{NL}}})$  for two different pivot scales,  $k_*$  and  $n_s = 0.96$ . The dashed line shows the maximal value of  $n_{f_{\text{NL}}}$  (and  $n_{\tau_{\text{NL}}}$ ), for which the approximation of Eq. (25) is correct.

PIXIE experiment [32],  $\ell_{\text{max}} = 84$  and  $w_\mu^{-1/2} = \sqrt{4\pi} \times 10^{-8}$ . We also approximate the variance of the  $C_\ell$ 's by

$$\begin{aligned} \sigma_{C_\ell^{\mu T}}^2 &= \langle (C_\ell^{\mu T})^2 \rangle - \langle C_\ell^{\mu T} \rangle^2 \\ &= \frac{1}{2\ell + 1} ((C_\ell^{\mu\mu} + C_\ell^{\mu\mu, N})(C_\ell^{TT} + C_\ell^{TT, N}) + (C_\ell^{\mu T})^2) \\ &\simeq \frac{1}{2\ell + 1} C_\ell^{TT} C_\ell^{\mu\mu, N} \end{aligned} \quad (25)$$

and

$$\sigma_{C_\ell^{\mu\mu}}^2 \simeq \frac{2}{2\ell + 1} (C_\ell^{\mu\mu, N})^2, \quad (26)$$

where we have used the fact that<sup>2</sup>

$$\begin{aligned} C_\ell^{TT} &\gg C_\ell^{TT, N}, & C_\ell^{\mu\mu, N} &\gg C_\ell^{\mu\mu} & \text{and} \\ C_\ell^{TT} C_\ell^{\mu\mu, N} &\gg (C_\ell^{\mu T})^2. \end{aligned} \quad (27)$$

The signal-to-noise ratio for  $n_{f_{\text{NL}}}$  at fixed  $f_{\text{NL}}^*$  is given by

$$\begin{aligned} \left( \frac{S}{N} \right)_{n_{f_{\text{NL}}}} &= n_{f_{\text{NL}}} / \sigma_{n_{f_{\text{NL}}}}(n_{f_{\text{NL}}}) \\ &= n_{f_{\text{NL}}} \sqrt{w_\mu \ln \left( \frac{\ell_{\text{max}}}{2} \right)} 11 \sqrt{\pi} \Delta_\zeta^3(k_p) f_{\text{NL}}^* \left( \frac{1}{\sqrt{2} k_*} \right)^{n_{f_{\text{NL}}}} \\ &\quad \times \left( \frac{1}{\sqrt{2} k_p} \right)^{n_s - 1} \left( \frac{1}{n_{f_{\text{NL}}} + n_s - 1} \right) \\ &\quad \times \left( \left( \ln \left( \frac{1}{\sqrt{2} k_*} \right) - \frac{1}{n_{f_{\text{NL}}} + n_s - 1} \right) [k_D^{n_{f_{\text{NL}}} + n_s - 1}]_{z_{\mu, f}}^{z_{\mu, i}} \right. \\ &\quad \left. + [\ln(k_D) k_D^{n_{f_{\text{NL}}} + n_s - 1}]_{z_{\mu, f}}^{z_{\mu, i}} \right), \end{aligned} \quad (28)$$

whereas the signal-to-noise ratio for  $n_{\tau_{\text{NL}}}$  at fixed  $\tau_{\text{NL}}^*$  is

$$\begin{aligned} \left( \frac{S}{N} \right)_{n_{\tau_{\text{NL}}}} &= n_{\tau_{\text{NL}}} 30 \pi w_\mu \Delta_\zeta^6(k_p) \tau_{\text{NL}}^* \ln^2 \left( \frac{k_{D, i}}{k_{D, f}} \right) \left( \ln \left( \frac{1}{\sqrt{2} k_*} \right) \right. \\ &\quad \left. - \frac{1}{n_{\tau_{\text{NL}}} + n_s - 1} + \frac{[\ln(k_D) k_D^{n_{\tau_{\text{NL}}} + n_s - 1}]_{z_{\mu, f}}^{z_{\mu, i}}}{[k_D^{n_{\tau_{\text{NL}}} + n_s - 1}]_{z_{\mu, f}}^{z_{\mu, i}}} \right) \\ &\quad \times \tilde{b}(n_{\tau_{\text{NL}}}, k_*). \end{aligned} \quad (29)$$

<sup>2</sup>Using the explicit expressions above, we find that this condition is verified, provided that  $(f_{\text{NL}}^* b)^2, \tau_{\text{NL}}^* \tilde{b} < 10^7 \ell^2$ . We consider the pivots  $k_* = 0.002 \text{ Mpc}^{-1}$  and  $k_* = 0.064 h \text{ Mpc}^{-1} \simeq 0.045 \text{ Mpc}^{-1}$ . The former corresponds to the pivot  $k_p$  of the primordial spectrum and the latter to the best pivot value from Ref. [26]. For  $\tau_{\text{NL}}^* \sim (f_{\text{NL}}^*)^2 \sim 10^4$  and  $\ell \sim 10^2$ , we find that the approximation of Eq. (25) is valid for  $n_{f_{\text{NL}}}, n_{\tau_{\text{NL}}} \lesssim (0.65-0.85)$  depending on the pivot  $k_*$ ; see Fig. 1, which presents the values of  $b$  and  $\tilde{b}$  as function of the indices  $n_{f_{\text{NL}}}$  and  $n_{\tau_{\text{NL}}}$  for the two pivots. One should be aware that in the multiple field case,  $\tau_{\text{NL}}^*$  is larger than  $((6/5)f_{\text{NL}}^*)^2$ , so the approximation becomes worse. In general, it seems reasonable to trust our estimation up to  $n_{f_{\text{NL}}}, n_{\tau_{\text{NL}}} \simeq 0.5$ .

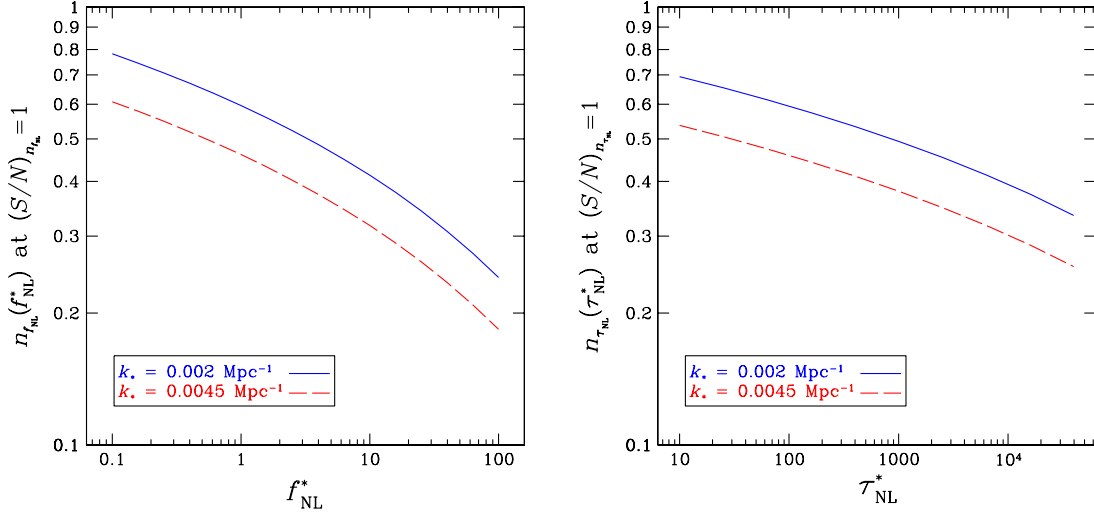


FIG. 2 (color online). Left: The spectral index  $n_{f_{NL}}^*$  as a function of  $f_{NL}^*$  at  $(S/N)_{n_{f_{NL}}} = 1$ . Right: The spectral index  $n_{\tau_{NL}}^*$  as a function of  $\tau_{NL}^*$  at  $(S/N)_{n_{\tau_{NL}}} = 1$ . Both plots are made for two different pivot scales  $k_*$ , using  $k_p = 0.002 \text{ Mpc}^{-1}$  and  $n_s = 0.96$  for PIXIE.

The left plot of Fig. 2 shows  $n_{f_{NL}}(f_{NL}^*)$  at  $(S/N)_{n_{f_{NL}}} = 1$ . An amplitude  $f_{NL}^* \lesssim 10^2$  enables us to detect  $n_{f_{NL}} \gtrsim 0.3$ , at least with the PIXIE experiment. Notice also that the dependence on the choice of  $k_*$  is relatively low. The right plot of Fig. 2 shows  $n_{\tau_{NL}}(\tau_{NL}^*)$  at  $(S/N)_{n_{\tau_{NL}}} = 1$ . Values of  $\tau_{NL}^* \lesssim 10^5$  enable us to detect  $n_{\tau_{NL}} \gtrsim 0.3$ , again with the PIXIE experiment.

In the single-field case, we can use either the temperature- $\mu$  distortion correlation  $C^{\mu T}$  or the  $\mu$ -distortion self-correlation  $C^{\mu\mu}$  to measure  $n_{f_{NL}}$ . As shown in Fig. 3,  $C^{\mu T}$  allows us to detect lower values of  $n_{f_{NL}}$ .

### III. HALO BIAS

Let us now turn to the effect of running NG parameters on the halo bias [17,20–22,25,33]. The halo bias power spectrum with Gaussian initial conditions can be simply expressed at lowest order in terms of a linear (Eulerian) bias parameter

$$P_h(k) = (b_1^E)^2 P_m(k), \quad (30)$$

where  $P_m(k)$  is the dark matter power spectrum. The effect of primordial non-Gaussianity on the halo bias can be accurately predicted from a peak-background split [33–37]. As shown in Ref. [33], the non-Gaussian contribution to the linear bias induced by a nonzero primordial  $N$ -point function is

$$\Delta b_1(k) = \frac{4}{(N-1)!} \frac{\mathcal{F}_s^{(N)}(k, z)}{\mathcal{M}_s(k, z)} \left[ b_{N-2} \delta_c + b_{N-3} \left( N-3 + \frac{d \ln \mathcal{F}_s^{(N)}(k, z)}{d \ln \sigma_s} \right) \right], \quad (31)$$

where  $b_N$  are Lagrangian bias parameters,  $\delta_c \sim 1.68$  is the critical threshold for (spherical) collapse, and  $\sigma_s$  is the root-mean-square (rms) variance of the density field at redshift  $z$  smoothed on the (small) scale  $R_s$  of a halo. While this expression assumes a universal mass function, it can be generalized to take into account deviations from universality in actual halo mass functions [37].

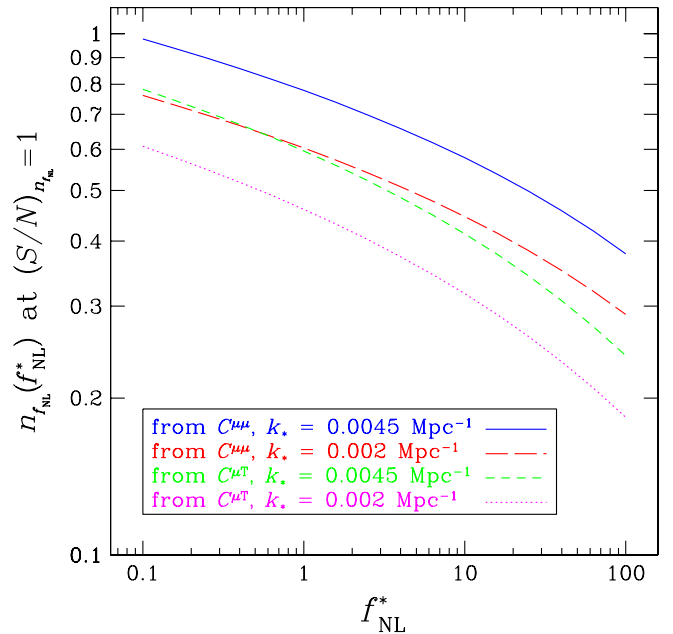


FIG. 3 (color online). Using the temperature- $\mu$ -distortion correlation  $C^{\mu T}$  allows to detect lower values of  $n_{f_{NL}}$  than using the  $\mu$ -distortion self-correlation  $C^{\mu\mu}$  in the single field case. The spectral index  $n_{f_{NL}}$  at  $(S/N)_{n_{f_{NL}}}$  is shown for two different pivot scales  $k_*$ , using  $k_p = 0.002 \text{ Mpc}^{-1}$  and  $n_s = 0.96$  for PIXIE.

The linear matter density contrast  $\delta_{\vec{k}}(z)$  is related to the curvature perturbation  $\Phi_{\vec{k}}$  during matter domination via the Poisson equation. The latter can be expressed as the Fourier space relation  $\delta_{\vec{k}}(z) = \mathcal{M}(k, z)\Phi_{\vec{k}}$ , where

$$\mathcal{M}(k, z) \equiv \frac{2}{3} \frac{D(z)}{\Omega_m H_0^2} T(k) k^2. \quad (32)$$

Here,  $T(k)$  is the matter transfer function,  $\Omega_m$  and  $H_0$  are the matter density in critical units and the Hubble rate today, and  $D(z)$  is the linear growth rate.  $\mathcal{M}_s$  is a shorthand for  $\mathcal{M}(k, z)W(kR_s)$ , where  $W(kR_s)$  is a spherically symmetric window function (we adopt a top-hat filter throughout this paper). Furthermore,

$$\begin{aligned} \mathcal{F}_s^{(N)}(k, z) &= \frac{1}{4\sigma_s^2 P_\phi(k)} \left[ \prod_{i=1}^{N-2} \int \frac{d^3 k_i}{(2\pi)^3} \mathcal{M}_s(k_i, z) \right] \mathcal{M}_s(q, z) \\ &\times \xi_\Phi^{(N)}(\vec{k}_1, \dots, \vec{k}_{N-2}, \vec{q}, \vec{k}) \end{aligned} \quad (33)$$

is a projection factor whose  $k$  dependence is dictated by the exact shape of the  $N$ -point function  $\xi_\Phi^{(N)}$  of the gravitational potential. For the local constant- $f_{\text{NL}}$  model, the factor  $\mathcal{F}_s^{(3)}$  is equal to  $f_{\text{NL}}$  in the low- $k$  limit (squeezed limit), so that the logarithmic derivative of  $\mathcal{F}_s^{(N)}$  with respect to the rms variance  $\sigma_s$  of the small-scale density field vanishes on large scales. However, this does not hold for scale-dependent primordial non-Gaussianity. In this case, we use Eqs. (4) and (6) for the bispectrum and trispectrum to evaluate the derivative of  $\mathcal{F}_s^{(N)}$  with respect to  $\sigma_s$ .

For generic primordial three- and four-point functions, the non-Gaussian halo power spectrum reads

$$\begin{aligned} P_h(k) &= \left[ (b_1^E)^2 + 4b_1^E b_1 \delta_c \frac{\mathcal{F}(n_{f_{\text{NL}}}, M)}{\mathcal{M}_R(k)} \right. \\ &+ \frac{25}{27} b_1^E \left[ b_2 \delta_c \sigma_R^2 + b_1 \left( 1 + \frac{d \ln \mathcal{T}_1}{d \ln \sigma_R} \right) \right] \\ &\times \frac{\mathcal{T}_1(n_{\tau_{\text{NL}}}, M)}{\mathcal{M}_R(k)} + \frac{25}{9} b_1^2 \delta_c^2 \frac{\mathcal{T}_2(n_{\tau_{\text{NL}}}, M)}{\mathcal{M}_R^2(k)} \left. \right] P_m(k), \end{aligned} \quad (34)$$

where, on large scales, the last term in the square brackets can generate stochasticity between the halo and mass density fields if  $\tau_{\text{NL}}$  is different from  $(6f_{\text{NL}}/5)^2$  [38–41]. We have defined the quantities

$$\mathcal{F}(n_{f_{\text{NL}}}, M) = \frac{1}{\sigma_R^2} \int \frac{dq}{2\pi^2} q^2 \mathcal{M}_R^2(q) P(q) f_{\text{NL}}(q), \quad (35)$$

$$\begin{aligned} \mathcal{T}_1(n_{\tau_{\text{NL}}}, M) &= \frac{6}{\sigma_R^4} \int \frac{d^3 q_1 d^3 q_2}{(2\pi)^6} \mathcal{M}_R(q_1) \mathcal{M}_R(q_2) \mathcal{M}_R(q_{12}) \\ &\times P(q_1) P(q_2) \tau_{\text{NL}}(q_1, q_{12}), \end{aligned} \quad (36)$$

$$\begin{aligned} \mathcal{T}_2(n_{\tau_{\text{NL}}}, M) &= \frac{1}{\sigma_R^4} \int \frac{dq_1 dq_2}{(2\pi^2)^2} q_1^2 q_2^2 \mathcal{M}_R^2(q_1) \mathcal{M}_R^2(q_2) P(q_1) \\ &\times P(q_2) \tau_{\text{NL}}(q_1, q_2). \end{aligned} \quad (37)$$

We have used the definitions in Eqs. (8) and (9) to obtain these expressions. We have also emphasized the dependence on the parameters  $n_{f_{\text{NL}}}$  and  $n_{\tau_{\text{NL}}}$ , as well as the halo mass  $M$  which, for the top-hat filter, is related to the smoothing radius  $R$  through  $R = (3M/4\pi)^{1/3}$ . The values of  $f_{\text{NL}}^*$  and  $\tau_{\text{NL}}^*$  at the pivot wave number  $k_* = 0.045 \text{ Mpc}^{-1}$  are assumed to be known. In the particular case of scale-independent  $f_{\text{NL}}$  and  $\tau_{\text{NL}}$ , i.e.,  $n_{f_{\text{NL}}} = n_{\tau_{\text{NL}}} = 0$ , we recover the expressions given in Refs. [38,41].

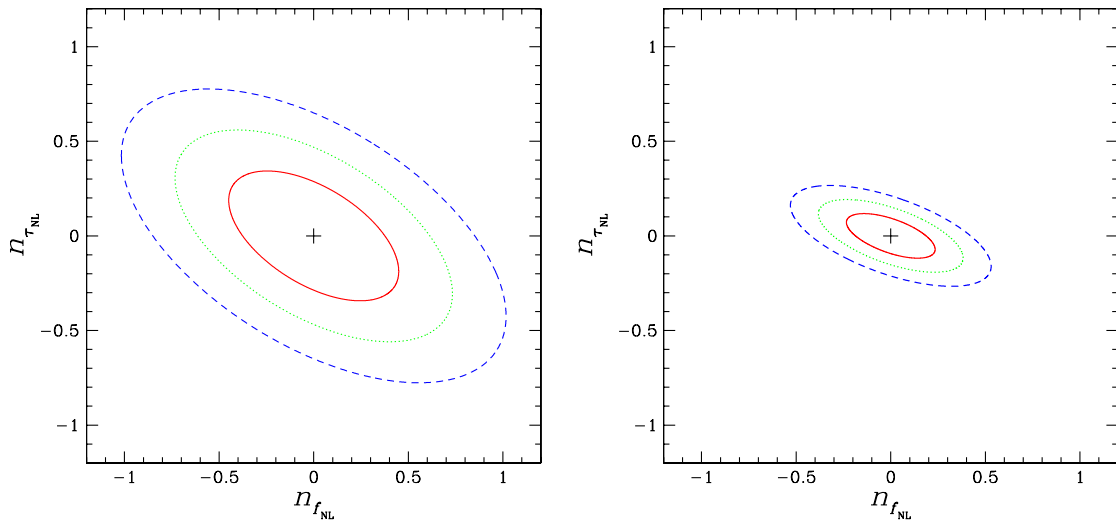


FIG. 4 (color online). Confidence ellipses obtained by the population of tracers considered with halos with mass larger than  $M = 10^{13} M_\odot/h$ , assuming  $f_{\text{NL}}^* = 20$  and  $\tau_{\text{NL}}^* = 5 \times 10^3$  (left) and  $f_{\text{NL}}^* = 50$  and  $\tau_{\text{NL}}^* = 5 \times 10^4$  (right).

In order to assess the ability of forthcoming experiments to probe the scale dependence of the nonlinearity parameters  $f_{\text{NL}}$  and  $\tau_{\text{NL}}$  through a measurement of the large-scale bias, we use the Fisher information content on  $f_{\text{NL}}$  and  $\tau_{\text{NL}}$  (see, e.g., Refs. [17,20–23,25] for application to the scale dependence of  $f_{\text{NL}}$ ) in the two-point statistics of halos and dark matter in Fourier space.

Computing the Fisher information requires knowledge of the covariance matrix of the halo samples:

$$C_h(k, M, z) = b^2(k, M, z)P_m(k) + \frac{1}{\bar{n}}, \quad (38)$$

where  $\bar{n}$  is the mean number density of the survey. In order to constrain  $n_{f_{\text{NL}}}$  and  $n_{\tau_{\text{NL}}}$ , we assume that we have already measured  $f_{\text{NL}}^*$  and  $\tau_{\text{NL}}^*$ . Moreover, since we are interested in investigating the possibility of a detection of the spectral indices, we take  $n_{f_{\text{NL}}} = n_{\tau_{\text{NL}}} = 0$  throughout as fiducial values. The Fisher matrix is defined as follows:

$$\mathcal{F}_{ij} = V_{\text{surv}} f_{\text{sky}} \int \frac{dk k^2}{2\pi^2} \frac{1}{2C_h^2} \frac{\partial C_h}{\partial \theta_i} \frac{\partial C_h}{\partial \theta_j}, \quad (39)$$

where  $\theta_i$  are the parameters whose error we wish to forecast,  $V_{\text{surv}}$  is the surveyed volume, and  $f_{\text{sky}}$  is the fraction of the sky observed. The integral over the momenta runs from  $k_{\text{min}} = 2\pi/(V_{\text{surv}})^{1/3}$  to  $k_{\text{max}} = 0.03 \text{ Mpc}^{-1}/h$ , above which the non-Gaussian bias becomes smaller than contributions from second-order bias and nonlinear gravitational evolution. For illustration, we adopt the specifications of a wide-angle, high-redshift survey such as BigBOSS or EUCLID:  $V_{\text{surv}} f_{\text{sky}} = 50 \text{ Gpc}^3/h^3$  at median redshift  $z = 0.7$ . Furthermore, we ignore redshift evolution and assume that all the surveyed volume is at the median redshift.

We compute the uncertainties on  $n_{f_{\text{NL}}}$  and  $n_{\tau_{\text{NL}}}$  from a single population of tracers consisting of all halos of mass larger than  $10^{13} M_{\odot}/h$ . Computing the Lagrangian bias factors from a Sheth-Tormen mass function [42] leads to linear and quadratic Lagrangian biases  $b_1 = 0.7$  and  $b_2 = -0.4$ . We take the number density to be  $\bar{n} = 10^{-4} \text{ Mpc}^3/h^3$ .

Figure 4 shows the resulting 68%, 95% and 99% confidence contours for the parameters  $n_{f_{\text{NL}}}$  and  $n_{\tau_{\text{NL}}}$  when we assume two different combinations of  $f_{\text{NL}}^*$  and  $\tau_{\text{NL}}^*$ . The  $1\sigma$  errors are displayed in Table I. In the specific case in which only one degree of freedom is responsible for the perturbations, we can use the relation  $\tau_{\text{NL}}(k_i, k_j) = \frac{36}{25} f_{\text{NL}}(k_i) f_{\text{NL}}(k_j)$ , which leaves us with only one param-

TABLE I.  $1\sigma$  errors for the population considered in the two different sets of  $f_{\text{NL}}^*$  and  $\tau_{\text{NL}}^*$  in Fig. 4.

$f_{\text{NL}}^*$	$\tau_{\text{NL}}^*$	$\sigma_{n_{f_{\text{NL}}}}$	$\sigma_{n_{\tau_{\text{NL}}}}$
20	$5 \times 10^3$	0.30	0.23
50	$5 \times 10^4$	0.15	0.08

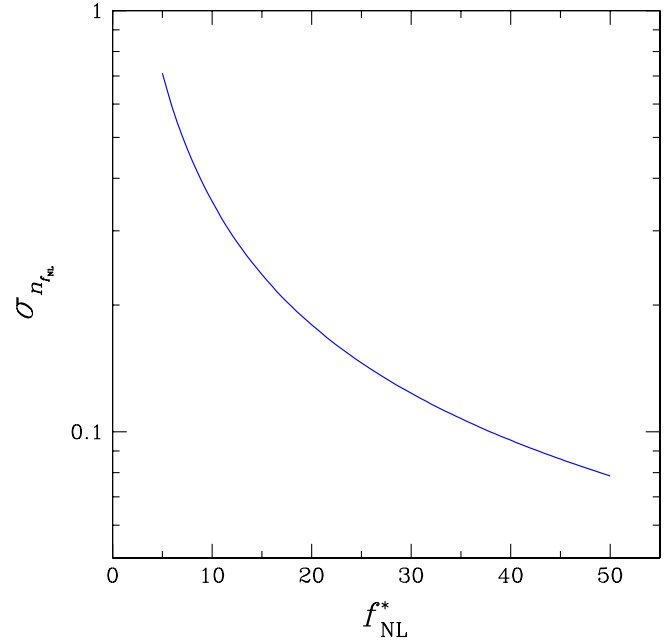


FIG. 5 (color online).  $1\sigma$  error predictions for  $n_{f_{\text{NL}}}$  as a function of  $f_{\text{NL}}^*$  at the pivot point  $k_* = 0.045 \text{ Mpc}^{-1}$  for the population considered in the case of single-field models.

ter,  $n_{f_{\text{NL}}}$ , describing the scale dependence of the primordial NG. The  $1\sigma$  error for  $n_{f_{\text{NL}}}$  as a function of  $f_{\text{NL}}^*$  is shown in Fig. 5. This result can be compared with those of previous work. For a fiducial value of  $f_{\text{NL}}^* = 50$  in particular, we find an error of  $\Delta n_{f_{\text{NL}}} \sim 0.2$  in the case of multifield models, and  $\Delta n_{f_{\text{NL}}} \sim 0.1$  in the case of single-field models. For single-field models, this is a factor of  $\mathcal{O}(3)$  lower than the forecast error found in Ref. [17] for a survey like EUCLID. We attribute this difference to the fact that we have considered the higher-order term  $\mathcal{O}(f_{\text{NL}}^2)$  in the halo bias, and to the parametrization  $f_{\text{NL}}(K) = f_{\text{NL}}(k_*) \times (K^{1/3}/k_*)^{n_{f_{\text{NL}}}}$  considered in Ref. [17] for the running of  $f_{\text{NL}}$ . In this regard, note that  $K \equiv k_1 k_2 k_3$  gives a contribution to the scaling of the external momentum, leading to a suppression (for a positive  $n_{f_{\text{NL}}}$ ) or enhancement (for a negative  $n_{f_{\text{NL}}}$ ) of the signal with respect to our parametrization in Eq. (8).<sup>3</sup> We have checked that, if we use the parametrization and restrict ourselves to the  $\mathcal{O}(f_{\text{NL}})$  contribution to the halo bias, we are able to reproduce their results. As noted in the Introduction, the parametrization used in this paper seems to be motivated by various theoretical predictions (see, for example, Refs. [14,25]).

<sup>3</sup>Determining  $n_{f_{\text{NL}}}$  through  $\mu$  distortion using the parametrization of Ref. [17] also leads to a deterioration of the  $S/N$  ratio. The parameter  $b$  is approximated by Eq. (17) with  $n_{f_{\text{NL}}}$  replaced by  $2n_{f_{\text{NL}}}/3$ . The correlation  $C^{\mu T}$  is decreased by a factor of about  $\exp(-cn_{f_{\text{NL}}})$ , with  $c \approx 3, 4$  for  $k_* = 0.002, 0.045 \text{ Mpc}^{-1}$ , respectively, relative to the parametrization in Eq. (8). Correspondingly, the error  $\sigma_{n_{f_{\text{NL}}}}$  is increased by about  $\frac{3}{2} \exp(cn_{f_{\text{NL}}})$ .

#### IV. CONCLUSION

Even a tiny level of non-Gaussianity in the cosmological perturbations can tell us a lot about the dynamics of the inflationary Universe. In this paper, we have focused on local non-Gaussianity, which is a generic prediction of multifield inflationary models where cosmological perturbations are sourced by light scalar fields other than the inflaton. We have considered the possibility that the nonlinear parameter  $f_{\text{NL}}$  is scale dependent and, extending the previous literature, we have also assumed that  $\tau_{\text{NL}}$  may be scale dependent. This is an unavoidable consequence when only a single field other than the inflaton generates the perturbation, as the spectral indices  $n_{f_{\text{NL}}}$  and  $n_{\tau_{\text{NL}}}$  are equal. We have considered two possible probes of a running non-Gaussianity. First, we have exploited the fact that future measurements of the CMB  $\mu$  distortion will be very sensitive to small scales, thereby enhancing the effect of a (blue) tilt of the

NG parameters. Second, we have assessed the ability of a large-scale galaxy survey to constrain the scale dependence of  $f_{\text{NL}}$  and  $\tau_{\text{NL}}$  imprinted in the non-Gaussian halo bias. Assuming the detection of a nonvanishing  $f_{\text{NL}}$  and  $\tau_{\text{NL}}$ , we find for both a CMB experiment like PIXIE and a large-scale survey like EUCLID that the spectral indices could be measured with an accuracy of  $\mathcal{O}(0.3)$  for  $f_{\text{NL}} = 20$  and  $\tau_{\text{NL}} = 5000$ . In the case of a measurement of the scale-dependent halo bias, this limit could be improved by suitably combining the information from several tracers (e.g., Ref. [43]).

#### ACKNOWLEDGMENTS

M.B. and V.D. are supported by the Swiss National Science Foundation (SNSF). H.P. and A.R. are supported by the Swiss National Science Foundation (SNSF) project ‘‘The non-Gaussian Universe’’ (Project No. 200021140236).

- 
- [1] For a review, see N. Bartolo, E. Komatsu, S. Matarrese, and A. Riotto, *Phys. Rep.* **402**, 103 (2004).
  - [2] E. Komatsu *et al.* (WMAP Collaboration), *Astrophys. J. Suppl. Ser.* **192**, 18 (2011).
  - [3] N. Dalal, O. Dore, D. Huterer, and A. Shirokov, *Phys. Rev. D* **77**, 123514 (2008).
  - [4] For a review, see V. Desjacques and U. Seljak, *Adv. Astron.* **2010**, 908640 (2010).
  - [5] P. Creminelli, *Phys. Rev. D* **85**, 041302 (2012).
  - [6] A. Kehagias and A. Riotto, *Nucl. Phys.* **B864**, 492 (2012); **B868**, 577 (2013).
  - [7] A. Slosar, C. Hirata, U. Seljak, S. Ho, and N. Padmanabhan, *J. Cosmol. Astropart. Phys.* **08** (2008) 031; N. Afshordi and A.J. Tolley, *Phys. Rev. D* **78**, 123507 (2008).
  - [8] J. Smidt, A. Amblard, C.T. Byrnes, A. Cooray, A. Heavens, and D. Munshi, *Phys. Rev. D* **81**, 123007 (2010).
  - [9] T. Suyama and M. Yamaguchi, *Phys. Rev. D* **77**, 023505 (2008).
  - [10] G. Tasinato, C. T. Byrnes, S. Nurmi, and D. Wands, *Phys. Rev. D* **87**, 043512 (2013).
  - [11] M. Biagetti, V. Desjacques, and A. Riotto, *arXiv:1208.1616* (to be published).
  - [12] X. Chen, *Phys. Rev. D* **72**, 123518 (2005).
  - [13] J. Khoury and F. Piazza, *J. Cosmol. Astropart. Phys.* **07** (2009) 026.
  - [14] C. T. Byrnes, M. Gerstenlauer, S. Nurmi, G. Tasinato, and D. Wands, *J. Cosmol. Astropart. Phys.* **10** (2010) 004.
  - [15] A. Riotto and M.S. Sloth, *Phys. Rev. D* **83**, 041301 (2011).
  - [16] C.T. Byrnes, K. Enqvist, S. Nurmi, and T. Takahashi, *J. Cosmol. Astropart. Phys.* **11** (2011) 011.
  - [17] E. Sefusatti, M. Liguori, A.P.S. Yadav, M.G. Jackson, and E. Pajer, *J. Cosmol. Astropart. Phys.* **12** (2009) 022.
  - [18] Q.-G. Huang, *J. Cosmol. Astropart. Phys.* **11** (2010) 026; **02** (2011) 01(E).
  - [19] Q.-G. Huang, *J. Cosmol. Astropart. Phys.* **12** (2010) 017.
  - [20] A. Becker, D. Huterer, and K. Kadota, *J. Cosmol. Astropart. Phys.* **01** (2011) 006.
  - [21] A. Becker, D. Huterer, and K. Kadota, *J. Cosmol. Astropart. Phys.* **12** (2012) 034.
  - [22] M. LoVerde, A. Miller, S. Shandera, and L. Verde, *J. Cosmol. Astropart. Phys.* **04** (2008) 014.
  - [23] T. Giannantonio and C. Porciani, *Mon. Not. R. Astron. Soc.* **422**, 2854 (2012).
  - [24] I. Agullo and S. Shandera, *J. Cosmol. Astropart. Phys.* **09** (2012) 007.
  - [25] S. Shandera, N. Dalal, and D. Huterer, *J. Cosmol. Astropart. Phys.* **03** (2011) 017.
  - [26] A. Becker and D. Huterer, *Phys. Rev. Lett.* **109**, 121302 (2012).
  - [27] E. Pajer and M. Zaldarriaga, *Phys. Rev. Lett.* **109**, 021302 (2012).
  - [28] J. Ganc and E. Komatsu, *Phys. Rev. D* **86**, 023518 (2012).
  - [29] J. Chluba and R. A. Sunyaev, *arXiv:1109.6552*.
  - [30] F. James, *Statistical Methods in Experimental Physics*, 2nd ed. (World Scientific, Singapore, 2006).
  - [31] S. Dodelson, *Modern Cosmology* (Academic Press, New York, 2003).
  - [32] A. Kogut *et al.*, *J. Cosmol. Astropart. Phys.* **07** (2011) 025.
  - [33] V. Desjacques, D. Jeong, and F. Schmidt, *Phys. Rev. D* **84**, 063512 (2011).
  - [34] A. Slosar, *J. Cosmol. Astropart. Phys.* **03** (2009) 004.
  - [35] F. Schmidt and M. Kamionkowski, *Phys. Rev. D* **82**, 103002 (2010).



- [36] K.M. Smith, S. Ferraro, and M. LoVerde, *J. Cosmol. Astropart. Phys.* **03** (2012) 032.
- [37] R. Scoccimarro, L. Hui, M. Manera, and K. C. Chan, *Phys. Rev. D* **85**, 083002 (2012).
- [38] J.-O. Gong and S. Yokoyama, *Mon. Not. R. Astron. Soc.* **417**, L79 (2011).
- [39] D. Tseliakhovich, C.M. Hirata, and A. Slosar, *Phys. Rev. D* **82**, 043531 (2010).
- [40] D. Baumann, S. Ferraro, D. Green, and K.M. Smith, [arXiv:1209.2173](https://arxiv.org/abs/1209.2173).
- [41] S. Yokoyama and T. Matsubara, *Phys. Rev. D* **87**, 023525 (2013).
- [42] R.K. Sheth, H.J. Mo, and G. Tormen, *Mon. Not. R. Astron. Soc.* **323**, 1 (2001).
- [43] N. Hamaus, U. Seljak, and V. Desjacques, *Phys. Rev. D* **84**, 083509 (2011).